Volume Integral Equation Based Diakoptic Method for Electromagnetic Modeling

Elene Chobanyan, *Student Member, IEEE*, Dragan I. Olćan, *Member, IEEE*,
Milan M. Ilić, *Member, IEEE*, and Branislav M. Notaroš, *Fellow, IEEE*

***Abstract*—A novel diakoptic method based on volume integral equation (VIE) modeling of subsystems is proposed for 3-D electromagnetic analysis. The theoretical foundation of the method are the surface and volume equivalence principles, as it combines the VIE and surface integral equation (SIE) formulations, in conjunction with the method of moments (MoM). The method breaks the original structure into a number of non-overlapping closed-region subsystems that contain inhomogeneous dielectric materials and an open-region subsystem. Each subsystem is analyzed completely independently applying the double-higher-order large-domain Galerkin generalized MoM-VIE-SIE (VSIE) or MoM-SIE solvers. The final solution is obtained from diakoptic matrices expressing linear relations between the electric and magnetic equivalent surface current coefficients on diakoptic surfaces. The proposed VSIE-diakoptic method is validated, evaluated, and discussed in several characteristic examples. The examples demonstrate that the diakoptic method substantially increases the efficiency of the conventional MoM-VIE approach. When compared to the pure MoM-VIE double-higher-order technique, the diakoptic approach enables very considerable accelerations and memory savings, while fully preserving the accuracy of the analysis.**

***Index Terms*—Numerical techniques, electromagnetic analysis, diakoptic analysis, volume integral equation, surface equivalence principle, method of moments, domain decomposition, higher order modeling.**

I. Introduction

THE method of moments (MoM) in conjunction with the volume integral equation (VIE) formulation is a well-established approach to computational electromagnetic (CEM) modeling of three-dimensional (3-D) dielectric structures, as well as composite dielectric and metallic structures [1]. The MoM-VIE methodology is especially suitable in cases involving inhomogeneous and complex dielectric materials. In such cases, it is a natural choice and is preferred over the overall more frequently used MoM methodology based on the surface integral equation (SIE) approach [2]. In many other cases, the MoM-VIE approach provides a useful alternative to the MoM-SIE modeling and on par or sometimes a more efficient solution. In fact, there has recently been a great renewed interest in VIE modeling in CEM and its applications, e.g., [3]-[5]. However, any increase in computational efficiency, in terms of either the computation time or the memory requirements, while preserving accuracy and robustness of this theoretically and conceptually very simple and elegant volumetric modeling technology, is always desired, especially if it can be done in a systematic, methodological fashion.

This paper proposes a novel diakoptic method based on VIE modeling of subsystems, as one possible strategy aimed at substantially enhancing the efficiency of the conventional MoM-VIE approach. The theoretical foundation of the method consists of the surface and volume equivalence principles. The numerical foundation of the method is a generalized MoM-VIE-SIE (VSIE) solver [6]-[9]. The diakoptic approach [10]-[14] solves a large and complex electromagnetic (EM) system as a linear combination of solutions of diakoptic subsystems, by means of matrix linear relations between coefficients in equivalent electric and magnetic surface current expansions on subsystem boundary surfaces (diakoptic surfaces).

Being based on the surface equivalence principle, the proposed diakoptic analysis is similar in spirit to the equivalence principle algorithm (EPA) [15]-[18] and the nested equivalence principle algorithm (NEPAL) [19], [20]. However, unlike in EPA, where the solution is based on establishing relations between the entire set of equivalent electric/magnetic currents of each domain with all the currents in all other domains and incident fields, matrix relations in diakoptics are established between electric and magnetic currents within each individual domain. Computation of these relations is solely based on manipulations with the current expansion coefficients. As such, it can be applied to the generalized MoM-VSIE method regardless of the geometry modeling (straight or curvilinear) and it can be implemented in already existing generalized MoM-VSIE codes with virtually no changes in those codes, except the partitioning. A difference is also that EPA methods introduce another set of

Manuscript first received April 19, 2015; revised and resubmitted November 7, 2015; revised June 25, 2016. This work was supported by the National Science Foundation under grants ECCS-1002385, ECCS-1307863, and AGS-1344862 and by the Serbian Ministry of Education, Science, and Technological Development under Grant TR-32005.

E. Chobanyan and B. M. Notaroš are with Colorado State University, Department of Electrical and Computer Engineering, Fort Collins, CO 80523-1373 USA (phone: 970-491-3537; fax: 970-491-2249; e-mail: elene.chobanyan@colostate.edu, notaros@colostate.edu).

D. I. Olćan is with University of Belgrade, School of Electrical Engineering, 11120 Belgrade, Serbia (e-mail: olcan@etf.rs).

M. M. Ilić is with University of Belgrade, School of Electrical Engineering, 11120 Belgrade, Serbia and with the Colorado State University, Department of Electrical and Computer Engineering, Fort Collins, CO 80523-1373, USA (e-mail: milanilic@etf.rs).

basis functions for connecting the regions, while the diakoptic approach works with the same basis functions as the MoM-SIE. While NEPAL solves a VIE, it is based solely on the representation of the scattered field by radiation of point sources, represented by multipoles, and it is not obvious if and how it could be applied to more general or arbitrary VIE elements and basis functions. On the other hand, the general diakoptic analysis can certainly be seen as belonging, in a broader sense, to the class of contemporary domain decomposition (DD) methods, including those based on the finite element method (FEM) [21]-[27] and those based on the finite difference frequency-domain and time-domain (FDFD and FDTD) methods [28], [29], as well as DD-SIE methods [30], [31].

In specific, the VSIE-diakoptic method divides the original structure into a number of non-overlapping closed-region subsystems, which generally contain inhomogeneous dielectric materials and are analyzed by the generalized MoM-VSIE solver, and an open-region subsystem that encloses the other subsystems and is analyzed using the MoM-SIE technique. Parts of the original problem are represented by matrix linear relations, and diakoptic coefficients are formally similar to voltages and currents at ports of a linear multiport network. Diakoptic surfaces may completely coincide with the SIE surfaces, and this paper explicitly considers only such situations in numerical examples. However, in other situations, SIE surfaces may be inside diakoptic surfaces, where they may be discretized by the pure MoM-SIE method, which would introduce non-diakoptic surface-current unknowns in the VSIE-diakoptic model. In all cases, the unknowns on diakoptic surfaces are the only unknowns in the final system of equations. Closed-region diakoptic subsystems in the model can, but do not need to, be the same. The implemented VSIE-diakoptic numerical discretization is based on the double-higher-order large-domain Galerkin-type MoM-VIE and MoM-SIE modeling described in detail in [6] and [7], respectively. The hybridization of the VIE and SIE methods which results in a generalized volume-surface integral equation (VIE-SIE or VSIE) method is done as outlined in [8], [9]. The basic theory and preliminary results of the VSIE-diakoptic analysis are presented in a summary form in [14].

One more interesting interpretation of the diakoptic method is in order here. Namely, as the relation between the equivalent sources at the diakoptic surface is linear and includes contributions of the excitations situated in the subsystem, it can be written in a formally identical matrix form as the Norton (or Thévenin) representation of a linear multiport network. It is, therefore, valid for any EM environment (system) in which the subsystem may be placed (and combined with other subsystems of the same or different form), and the proposed diakoptic analysis can be formally interpreted as being equivalent to Norton's theorem in circuit theory. However, the diakoptic approach features the full EM-field generalization of the Norton representation, where, in fact, each pair of electric and magnetic equivalent surface current coefficients on the diakoptic surface represents a generalized port, to which a multiport network analogy is then applied. So, the diakoptic approach is not a lumped-element approximation of EM fields, but rather a 3-D EM generalization, based on a rigorous Maxwell-type solver, of Norton's theorem.

The diakoptic method manipulates with linear relations between expansion coefficients for currents within a subsystem and equivalent currents at the diakoptic surface. Hence, results for electromagnetic subsystems once used in the diakoptic analysis can be stored for future reuse, with a minimum computational overhead. We can change one (or more) subsystems (e.g., change material composition, excitations, dimensions or placement of subcomponents, etc.) and rerun the analysis, to re-compute the diakoptic coefficients extremely expeditiously. For instance, if any part of the system is changed, only coefficients for that part have to be recalculated in the diakoptic model. This can be very beneficial to design and optimization procedures. Additionally, if the problem includes many identical subdomains, such as in analysis and design of antenna or scatterer arrays, the solution of one constitutive subsystem can be efficiently reused for congruent subsystems.

This paper has three principal goals. (1) It demonstrates that the proposed VSIE-diakoptic method substantially increases the efficiency of the conventional MoM-VIE approach, and this is the primary goal. When compared to the pure MoM-VIE technique implementing the same type of discretization (double-higher-order large-domain discretization in our case, i.e., [6]), the diakoptic approach enables very considerable accelerations and memory savings, while preserving the accuracy of the analysis. However, the paper does not claim that this is the only or the best strategy to enhance the efficiency of the conventional MoM-VIE method. (2) The paper also demonstrates that the general diakoptic methodology can effectively include VIE-based subsystems, and shows how that can be done. (3) Finally, the paper combines the general MoM-VIE methodology and the general DD methodology, which are two out of several general numerical methodologies in CEM. However, the paper does not speculate on comparisons in terms of capabilities and performance of the presented diakoptics-VIE approach with a possible contemporary DD-VIE approach.

The rest of the paper is organized as follows. Section II presents the theory and implementation of the novel VSIE-diakoptic method starting with the surface and volume equivalence principles and a set of VSIE equations for the unknown volume and surface equivalent currents. This also includes double-higher-order MoM-VSIE modeling of EM subsystems and diakoptic surfaces, derivation of linear relations between diakoptic coefficients, representation of EM subsystems by diakoptic matrices, and solution of the diakoptic matrix system. In Section III, the proposed VSIE-diakoptic method is validated, evaluated, and discussed in several characteristic examples.

II. Diakoptic Method Based on MoM-VSIE Modeling

A. Surface and Volume Equivalence Principles

In the diakoptic analysis, the EM system is subdivided into

subsystems by virtue of the surface equivalence principle [32]. For the clarity of explanation, we consider a single domain v, bounded by a closed surface S, as depicted in Fig. 1(a), so two subsystems, v and its exterior. According to this principle, the electric and magnetic fields $\mathbf{E}$ and $\mathbf{H}$ everywhere can be uniquely evaluated by knowing electric and magnetic tangential fields $\mathbf{E}_S$ and $\mathbf{H}_S$ at S.

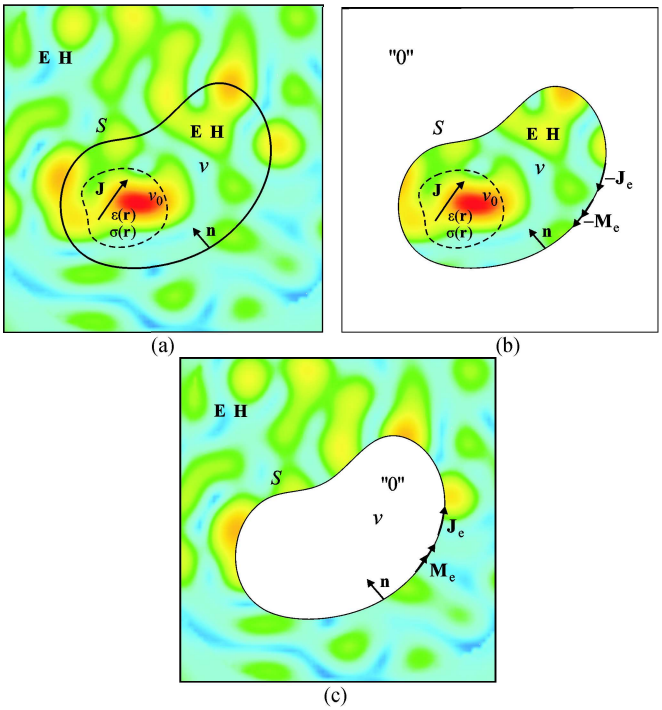

Fig. 1. Illustration of the surface and volume equivalence principles, as the theoretical foundation of the VSIE-diakoptic approach to electromagnetic analysis: (a) original EM system, divided into two subsystems by a closed surface S (diakoptic surface), on which equivalent surface currents are placed in order to radiate the actual fields, (b) equivalent interior problem, which includes an inhomogeneous dielectric body taken into account by the radiation of equivalent volume currents, and (c) equivalent exterior problem (with original fields outside and zero field inside S).

Let us assume that interior impressed volume electric currents of density $\mathbf{J}$ exist only in a domain v_0, which is a part of v. For example, these currents can represent an actual volume current distribution of a dielectric body located inside v. The fields $\mathbf{E}$ and $\mathbf{H}$ can be obtained as being radiated by fictitious electric and magnetic equivalent surface currents whose density vectors are given by $\mathbf{J}_e = -\mathbf{n}\times\mathbf{H}_S$ and $\mathbf{M}_e = \mathbf{n}\times\mathbf{E}_S$, where $\mathbf{n}$ stands for a normal unit vector on S, directed toward the interior region, as shown in Fig. 1(a). As a result of subtraction of the equivalent currents and their fields from the original problem, the fields $\mathbf{E}$ and $\mathbf{H}$ in v remain unchanged, while the fields in the exterior region are annihilated, Fig. 1(b). The surface equivalence principle for the exterior region is established in the analogous way, Fig. 1(c).

Assume now that the domain v_0 in Fig. 1(a) actually represents an arbitrarily shaped inhomogeneous dielectric body, with the permittivity $\varepsilon(\mathbf{r})$ and conductivity $\sigma(\mathbf{r})$ of the dielectric material being known functions of position (i.e., the vector $\mathbf{r}$), while the permeability at all points is μ_0. In accordance to the volume equivalence principle [32], the dielectric inhomogeneity can be taken into account by the radiation of volumetric electric currents of density $\mathbf{J}$, which we can consider as the impressed sources when applying the surface equivalence principle, in Fig. 1. The constitutive (material) relationship for the total electric field at each point of the domain v_0 and the tangential total electric and magnetic field boundary conditions on the surface S yield

$$\mathbf{E}\left(\mathbf{D},\mathbf{J}_e,\mathbf{M}_e\right)+\mathbf{E}^{\text{exc}} = \mathbf{D}/\varepsilon_c \tag{1}$$

$$\mathbf{n}\times\left(\mathbf{E}\left(\mathbf{D},\mathbf{J}_e,\mathbf{M}_e\right)+\mathbf{E}^{\text{exc}}\right)=0 \tag{2}$$

$$\mathbf{n}\times\left(\mathbf{H}\left(\mathbf{D},\mathbf{J}_e,\mathbf{M}_e\right)+\mathbf{H}^{\text{exc}}\right)=0 \tag{3}$$

where $\mathbf{E}\left(\mathbf{D},\mathbf{J}_e,\mathbf{M}_e\right)$ and $\mathbf{H}\left(\mathbf{D},\mathbf{J}_e,\mathbf{M}_e\right)$ are field vectors due to volumetric electric current density and surface electric and magnetic currents, $\mathbf{D}$ is the equivalent electric displacement (or flux density) vector, and ε_c is the equivalent complex permittivity of the material at that point, while $\mathbf{E}^{\text{exc}}$ and $\mathbf{H}^{\text{exc}}$ are excitation electric and magnetic fields resulting from arbitrarily positioned sources inside and/or outside of v. The vectors $\mathbf{J}$ and $\mathbf{D}$ are related to each other as

$$\mathbf{J} = \mathrm{j}\omega C\mathbf{D},\quad C=\frac{\varepsilon_c-\varepsilon_0}{\varepsilon_c},\quad \varepsilon_c=\varepsilon-\mathrm{j}\frac{\sigma}{\omega}, \tag{4}$$

with ω being the angular frequency of $\mathbf{E}^{\text{exc}}$ (time-harmonic convention $e^{\mathrm{j}\omega t}$ is used) and C the electric contrast (with respect to the surrounding medium) at each point of the object. Given the integral expressions for the fields in terms of sources $\mathbf{E}\left(\mathbf{D},\mathbf{J}_e,\mathbf{M}_e\right)$ and $\mathbf{H}\left(\mathbf{D},\mathbf{J}_e,\mathbf{M}_e\right)$ [6], [7], [14], (1)–(3) represent a system of three coupled electric/magnetic field integral VSIE equations with the sources $\mathbf{D}$, $\mathbf{J}_e$, and $\mathbf{M}_e$ as unknown quantities; we discretize and solve this system using the MoM.

B. Double-Higher-Order MoM-VSIE Discretization

The VSIE-diakoptic method is based on the double-higher-order (in both geometrical and current approximation) MoM modeling. This facilitates utilization of large curved volume and surface elements. Volume elements are Lagrange-type curved hexahedra of geometrical orders K_u, K_v, and K_w ($K_u, K_v, K_w \geq 1$), shown in Fig. 2(a). Within each element, the vector $\mathbf{D}$ is expanded via divergence-conforming hierarchical polynomial vector basis functions in parametric coordinates u, v, and w with arbitrary current-approximation orders N_u, N_v, and N_w ($N_u, N_v, N_w \geq 1$) [6], [14]. In the MoM-SIE discretization, modeling of S is carried out using Lagrange generalized curved quadrilateral elements of geometrical orders K_u and K_v ($K_u, K_v \geq 1$), in

Fig. 2(b), with the currents $\mathbf{J}_e$ and $\mathbf{M}_e$ over the patches being approximated by divergence-conforming hierarchical polynomial vector bases with orders N_u and N_v ($N_u, N_v \geq 1$) [7]. The K and N orders in one VIE or SIE element can be adopted completely independently from each other. All orders in different elements are also adopted at will, and there is no required connection between VIE and SIE orders. In the hybrid MoM-VSIE technique, the equations are tested using the Galerkin method.

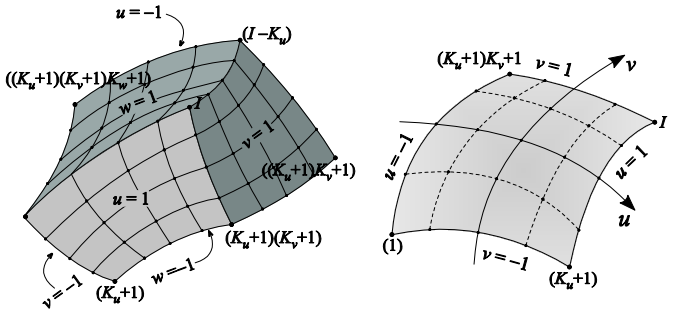

Fig. 2. Lagrange interpolation curved parametric elements for higher order VSIE-diakoptic analysis of the EM system in Fig. 1: (a) MoM-VIE generalized hexahedral element, determined by $I = (K_u + 1)(K_v + 1)(K_w + 1)$ interpolation nodes arbitrarily positioned in space, and (b) MoM-SIE generalized quadrilateral patch, defined by $I = (K_u + 1)(K_v + 1)$ nodes.

C. VSIE-Diakoptic Analysis

Discretizing (1)−(3) with the MoM, we obtain the following linear matrix system of equations:

$$\begin{array}{c} \\ N_S \\ N_V \\ N_S \end{array} \begin{array}{c} \begin{array}{cccccc} N_S & N_V & N_S & 1 & & 1 \\ \leftrightarrow & \leftrightarrow & \leftrightarrow & \leftrightarrow & & \leftrightarrow \end{array} \\ \updownarrow \begin{bmatrix} \mathbf{Z}_1 & \mathbf{Z}_2 & \mathbf{Z}_3 \\ \mathbf{Z}_4 & \mathbf{Z}_5 & \mathbf{Z}_6 \\ \mathbf{Z}_7 & \mathbf{Z}_8 & \mathbf{Z}_9 \end{bmatrix} \begin{bmatrix} \mathbf{j}_e \\ \mathbf{d} \\ \mathbf{m}_e \end{bmatrix} = \begin{bmatrix} \mathbf{v}_1 \\ \mathbf{v}_2 \\ \mathbf{v}_3 \end{bmatrix} \end{array} \tag{5}$$

where $[\mathbf{d}]$, $[\mathbf{j}_e]$, and $[\mathbf{m}_e]$ are column-matrices of unknown coefficients that approximate $\mathbf{D}$, $\mathbf{J}_e$, and $\mathbf{M}_e$, respectively, the generalized MoM-VSIE system matrix, $[\mathbf{Z}]$, is partitioned into sub-matrices $[\mathbf{Z}_k]$, $k = 1,2,...,9$, and $[\mathbf{v}_l]$, $l = 1,2,3$, form the excitation column-matrix. The N_V equations in (5) in the middle, N_S equations at the top, and N_S equations at the bottom are obtained by discretizing (1), (2), and (3), respectively. In particular, sub-matrices $[\mathbf{Z}_5]$ and $[\mathbf{Z}_m]$, $m = 1,3,7,9$ correspond to pure VIE and SIE discretizations, respectively, while $[\mathbf{Z}_n]$, $n = 2,4,6,8$, result from the generalized VSIE analysis [8], [9], [14].

A combined field integral equation (CFIE) formulation for the diakoptic surface (surface S in Fig. 1) can be obtained by multiplying the first N_S equations in (5) by α, and the last N_S equations by β, where we adopt $\alpha = 1$ and $\beta = -\sqrt{\mu_0 / \varepsilon_0}$. The CFIE formulation is used to avoid numerical instabilities at resonant frequencies of the diakoptic surface. Summing the new equations and moving all the terms associated with $[\mathbf{m}_e]$ to the right-hand side of the matrix equation results in

$$\begin{bmatrix} \alpha\mathbf{Z}_1 + \beta\mathbf{Z}_7 & \alpha\mathbf{Z}_2 + \beta\mathbf{Z}_8 \\ \mathbf{Z}_4 & \mathbf{Z}_5 \end{bmatrix} \begin{bmatrix} \mathbf{j}_e \\ \mathbf{d} \end{bmatrix} = -\begin{bmatrix} \alpha\mathbf{Z}_3 + \beta\mathbf{Z}_9 \\ \mathbf{Z}_6 \end{bmatrix} [\mathbf{m}_e] + \begin{bmatrix} \alpha\mathbf{v}_1 + \beta\mathbf{v}_3 \\ \mathbf{v}_2 \end{bmatrix}, \tag{6}$$

which allows establishing the following matrix linear relation:

$$\begin{bmatrix} \mathbf{j}_e \\ \mathbf{d} \end{bmatrix} = \begin{bmatrix} \mathbf{Y} \\ \mathbf{C} \end{bmatrix} [\mathbf{m}_e] + \begin{bmatrix} \mathbf{j}_0 \\ \mathbf{d}_0 \end{bmatrix}. \tag{7}$$

Based on (7), each of the subsystems in Fig. 1, i.e., the interior subsystem, for which $i = 1$, and the exterior subsystem, with $i = 2$, can be described by linear relations between coefficients $[\mathbf{j}_e]$ and $[\mathbf{m}_e]$ cast in matrix form as

$$[\mathbf{j}_{ei}] = [\mathbf{Y}_i][\mathbf{m}_{ei}] + [\mathbf{j}_{0i}], \quad i = 1,2 \tag{8}$$

where $[\mathbf{Y}_i]$ is the $N_S \times N_S$ diakoptic matrix $[\mathbf{Y}]$ in (7) for the i-th subsystem and $[\mathbf{j}_{0i}]$ is the $N_S \times 1$ column-matrix that contains coefficients representing the excitation in the subsystem. These matrices are numerically calculated by considering the coefficients $[\mathbf{m}_{ei}]$ as excitation and coefficients $[\mathbf{j}_{ei}]$ as the response – in the i-th subsystem. To obtain $[\mathbf{Y}_i]$, we excite the subsystem with only one coefficient of $[\mathbf{m}_{ei}]$ set to unity value and all other coefficients (as well as all excitations within the subsystem) set to zero; with an excitation by the j-th coefficient in $[\mathbf{m}_{ei}]$, the coefficients of $\mathbf{J}_e$ obtained using the generalized MoM-VSIE solver constitute the j-th column of $[\mathbf{Y}_i]$. From (7), we also obtain linear relations between $[\mathbf{m}_{e1}]$ and the VIE coefficients of $\mathbf{D}$ ($i = 1$), given by

$$[\mathbf{d}] = [\mathbf{C}][\mathbf{m}_{e1}] + [\mathbf{d}_0], \tag{9}$$

where the $N_V \times N_S$ diakoptic matrix $[\mathbf{C}]$ is filled column by column by computing the coefficients of $\mathbf{D}$ in the same MoM-VSIE analysis with $[\mathbf{Y}_i]$. For example, the solution for $[\mathbf{j}_e]$ and $[\mathbf{d}]$ of the matrix equation

$$\begin{bmatrix} \alpha\mathbf{Z}_1 + \beta\mathbf{Z}_7 & \alpha\mathbf{Z}_2 + \beta\mathbf{Z}_8 \\ \mathbf{Z}_4 & \mathbf{Z}_5 \end{bmatrix} \begin{bmatrix} \mathbf{j}_e \\ \mathbf{d} \end{bmatrix} = -\begin{bmatrix} \alpha\mathbf{Z}_3 + \beta\mathbf{Z}_9 \\ \mathbf{Z}_6 \end{bmatrix} \begin{bmatrix} 1 \\ 0 \\ \vdots \\ 0 \end{bmatrix} \tag{10}$$

forms the first column of matrix $[\mathbf{Y}\ \mathbf{C}]^T$ in (7), and so on. In

order to obtain the column matrix $[\mathbf{j}_0\ \mathbf{d}_0]^{\mathrm{T}}$, we solve the above matrix equation with $[\alpha\mathbf{v}_1+\beta\mathbf{v}_3\ \ \mathbf{v}_2]^{\mathrm{T}}$ on the right-hand side. While evaluating the diakoptic matrices, the matrix equation (6), i.e., the corresponding system of linear equations, is filled and LU (lower-upper) decomposed only once, and all the results are obtained with LU substitutions using different excitations. Namely, the main matrix on the left-hand side in (10) is LU factorized only once for multiple right-hand side vectors. Only forward/backward substitutions are applied in order to compute all the elements of the matrices [**Y**] and [**C**]. The complexity of LU is $O(N^3)$ and the complexity of a pair of forward/backward substitution is $O(N^2)$. With this, the advantage of utilizing a direct solver in the diakoptic approach is straightforward. In addition, the proposed VSIE-diakoptic approach can be combined with fast direct solvers [33]-[35]. An iterative solver can also be applied to subsystems, and the calculation in subsystems can be accelerated by fast methods [36]-[38].

Note that, since the matrix relation in (8) relates the electric surface current to the magnetic surface current, it could be considered as a form of the generalized impedance boundary condition (GIBC) [39], [40].

The solution of the original EM problem, in Fig. 1(a), is obtained by relating the diakoptic coefficients in expansions of the electric and magnetic equivalent surface currents on S (on the diakoptic surfaces, i.e., individual subsystem boundaries). These relations come out to be as simple as

$$[\mathbf{j}_{\mathrm{e}1}]=[\mathbf{j}_{\mathrm{e}2}]=[\mathbf{j}_{\mathrm{e}}] \text{ and } [\mathbf{m}_{\mathrm{e}1}]=[\mathbf{m}_{\mathrm{e}2}]=[\mathbf{m}_{\mathrm{e}}] \tag{11}$$

where the use is made of the facts that the signs of equivalent sources are opposite (based on the equivalence theorem) and so are the normal unit vector directions for the two neighboring subsystems. Diakoptic boundary conditions in (11) lead to stable VSIE-diakoptic CFIE solutions in all cases considered and all tests performed. Note that, theoretically, (11) is directly derived from the boundary conditions for both fields **H** and **E** at the diakoptic surface. Combining (8) and (11), the following diakoptic matrix system is obtained:

$$\left([\mathbf{Y}_1]-[\mathbf{Y}_2]\right)[\mathbf{m}_{\mathrm{e}}]=-[\mathbf{j}_{01}]+[\mathbf{j}_{02}] \tag{12}$$

which is solved for $[\mathbf{m}_{\mathrm{e}}]$ using a direct solver. Note that the matrices in (10) and (12) that need to be LU factorized (once) in the VSIE-diakoptic method are, in general, considerably smaller than the main matrix of the pure MoM-VIE technique implementing the same type of discretization. Once $[\mathbf{m}_{\mathrm{e}}]$ is found, $[\mathbf{j}_{\mathrm{e}}]$ and $[\mathbf{d}]$ can be computed from (8) and (9). Other quantities (e.g., electric and magnetic fields) can be calculated by post-processing of the coefficients by the MoM-VSIE code.

Note that when all the subsystems are isolated, there is one large exterior subsystem left to be solved by the MoM-SIE method. While this open-region subsystem relating all other subsystems becomes the bottleneck of the diakoptic method in such cases, the complexity of the method, associated with this subsystem only, is still significantly reduced in comparison with the pure MoM-SIE approach. From a purely mathematical standpoint (omitting EM theoretical background of the method, which plays a key role in the diakoptic technique), using the diakoptic approach we solve two systems with N_S and one with $(N_S/M+N_{\mathrm{V}})$ numbers of unknowns, respectively, with M being the number of congruent subdomains, as shown in (6)-(12) and Appendix I, instead of solving a system with $2N_S$ unknowns. Therefore, in diakoptics, the linear size of the system of equations associated with the global exterior subsystem is halved. In addition, theoretically, any matrix solver that allows us to obtain (6), (7), (8), and (9), and to solve (12) can be used with the diakoptic approach.

Note also that transition from (5) to (6)-(7) can be considered as the first step of static condensation [41]. However, further steps of static condensation would require one to substitute vector $[\mathbf{j}_{\mathrm{e}}\ \mathbf{d}]^{\mathrm{T}}$ back into (3) and proceed further with its solution. In the presented diakoptic technique, however, matrix equation (5) is created for each of the subsystems constituting interior and exterior of the diakoptic surface in Fig. 1, resulting into two matrix equations that are solved simultaneously for shared set of unknowns. Depending on the subsystem, equations (5) may or may not contain unknown coefficients $[\mathbf{d}]$. Using the surface equivalence principle and the procedure of decomposing the problem into subsystems that are solved independently, while taking into account their interaction via equivalent surface currents, we obtain two relations between $[\mathbf{j}_{\mathrm{e}}]$ and $[\mathbf{m}_{\mathrm{e}}]$ as shown in (8), and then solve the final system in (12) as explained above.

The presented diakoptic analysis is generalized to the case of an arbitrary number of subsystems. Equations (11) are valid for a common diakoptic boundary of two neighboring subsystems and the matrix representations (8) and (9) stand for each subsystem, so the diakoptic system has the same form, since each part of a diakoptic surface is always shared by two adjacent subsystems. As an illustration, consider three subsystems, denoted as Ω_1, Ω_2, and Ω_3, where the second and the third subsystem are in touch with the first, but not with each other. With the densities of the respective equivalent diakoptic current distributions being ($\mathbf{j}_{\mathrm{e}1}$, $\mathbf{m}_{\mathrm{e}1}$), ($\mathbf{j}_{\mathrm{e}2}$, $\mathbf{m}_{\mathrm{e}2}$), and ($\mathbf{j}_{\mathrm{e}3}$, $\mathbf{m}_{\mathrm{e}3}$), adjusting equations (11) and (12) leads to

$$\begin{bmatrix}\mathbf{j}_{\mathrm{e}2}\\ \mathbf{j}_{\mathrm{e}3}\end{bmatrix}=[\mathbf{j}_{\mathrm{e}1}]=[\mathbf{j}_{\mathrm{e}}] \text{ and } \begin{bmatrix}\mathbf{m}_{\mathrm{e}2}\\ \mathbf{m}_{\mathrm{e}3}\end{bmatrix}=[\mathbf{m}_{\mathrm{e}1}]=[\mathbf{m}_{\mathrm{e}}], \tag{13}$$

$$\left(\begin{bmatrix}\mathbf{Y}_2\\ \mathbf{Y}_3\end{bmatrix}-[\mathbf{Y}_1]\right)[\mathbf{m}_{\mathrm{e}}]=-\begin{bmatrix}\mathbf{j}_{02}\\ \mathbf{j}_{03}\end{bmatrix}+[\mathbf{j}_{01}], \tag{14}$$

where matrices $[\mathbf{Y}_i]$ and $[\mathbf{j}_{0i}]$ correspond to the i-th subsystem ($i=1,2,3$).

III. Numerical Examples and Discussion

A. Array of Homogeneous Dielectric Cubical Scatterers

As the first example of the application and validation of the VSIE-diakoptics approach, we consider an 8×8 array of homogeneous lossless dielectric cubes of edge lengths $a=\lambda_0/6$, where λ_0 is the free-space wavelength, and relative permittivity $\varepsilon_r=2.25$, excited by a uniform plane electromagnetic wave from the direction described by $\theta_{inc}=90°$ and $\phi_{inc}=0°$, as shown in Fig. 3(a). The surface-to-surface distance between neighboring cubes is $d=\lambda_0/6$, in both *x*- and *y*-directions.

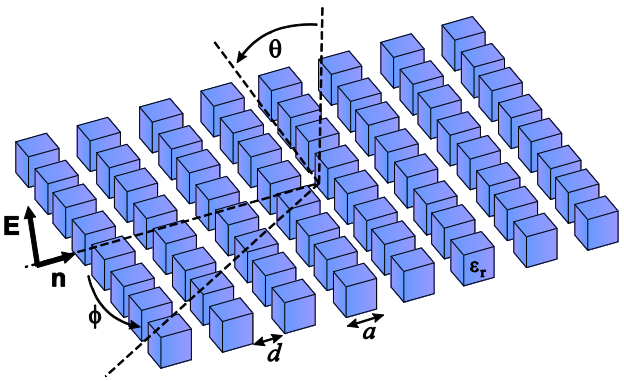

(a)

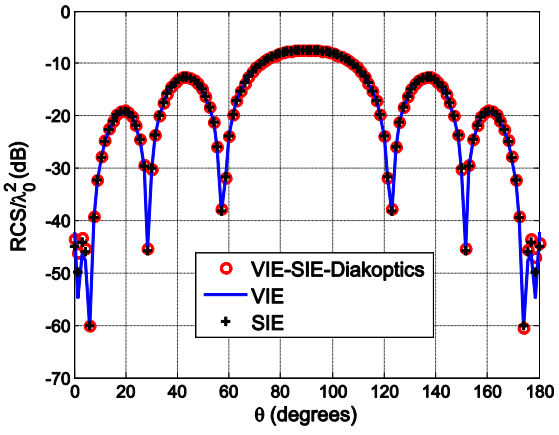

(b)

Fig. 3. (a) Array of homogeneous dielectric cubical scatterers excited by a uniform plane electromagnetic wave ($\theta_{inc}=90°$, $\phi_{inc}=0°$) and (b) normalized bistatic radar cross section (RCS) of the array in the $\phi=0°$ cut, computed by the proposed VSIE-diakoptic method, by the pure MoM-VIE technique [6], and the pure MoM-SIE technique [7].

For the diakoptic analysis, the system in Fig. 3(a) is split into 65 diakoptic subsystems: 64 interior VSIE subsystems coinciding with dielectric cubes and a free-space exterior SIE subsystem, which is in touch with all VSIE subsystems. A single VIE element is used for every cubical diakoptic subsystem, and the orders are adopted to be $K_u=K_v=K_w=1$ and $N_u=N_v=N_w=3$. Each cubical diakoptic surface is modeled by six SIE patches with $K_u=K_v=1$ and $N_u=N_v=2$. The number of VIE unknowns per subsystem is $N_V=108$ and the total number of diakoptic unknowns (summing the unknowns for all diakoptic surfaces) amounts to $2N_S=6{,}144$, which results in a total of $N_{tot}^{Dia}=6{,}252$ unknowns and $T_{tot}^{Dia}=98\,s$ of computation time for the analysis. In all computations presented in this paper, no parallelization or EM system symmetries are used. All computations are performed on an Intel® Core™2 Quad CPU Q9550 at 2.83 GHz, with 8 GB RAM, under 64-bit Windows 7 operating system. Shown in Fig. 3(b) is the normalized bistatic radar cross section (RCS) of the array in a plane defined by $\phi=0°$. A comparison is made between the diakoptic solution and the results obtained by the pure MoM-VIE method (with LU decomposition) [6], which require $N_{tot}^{VIE}=6{,}912$ unknowns and $T_{tot}^{VIE}=439\,s$ of computation time, and an excellent agreement is observed. In this example, the advantage of the diakoptic approach is not so much in the reduction of the number of unknowns, but of the computation time (about 4.5 times). Moreover, the computer memory (RAM) consumption is $M_{tot}^{Dia}=151\,MB$ for the VSIE-diakoptic method (note that in the diakoptic approach, the largest matrix equation that has to be solved is of the size N_S) and $M_{tot}^{VIE}=764\,MB$ for the MoM-VIE method. To validate the diakoptic solution further, Fig. 3(b) also shows its excellent agreement with the RCS computed by means of the pure MoM-SIE method (with LU decomposition) [7], which takes $N_{tot}^{SIE}=6{,}144$ unknowns, $T_{tot}^{SIE}=170\,s$ of computation time, and $M_{tot}^{SIE}=604\,MB$ of RAM.

B. Array of Homogeneous Dielectric Spherical Scatterers

As an example of curved structures, we replace the cubical scatterers in Fig. 3(a) by spherical ones, as portrayed in Fig. 4(a), where $a=\lambda_0/2.31$ (sphere diameter), $d=\lambda_0/4.29$, $\varepsilon_r=4$, $\theta_{inc}=90°$, and $\phi_{inc}=0°$. Each diakoptic subsystem, in spite of curvature, is again represented using a single VIE generalized hexahedron with $K_u=K_v=K_w=2$ and $N_u=N_v=N_w=4$, bounded by a diakoptic surface constructed from six SIE generalized quadrilaterals with $K_u=K_v=2$ and $N_u=N_v=2$, so the numbers of unknowns are $N_V=240$, $2N_S=6{,}144$, and $N_{tot}^{Dia}=6{,}384$, computation time is $T_{tot}^{Dia}=174\,s$, and computer memory consumption is $M_{tot}^{Dia}=152\,MB$. The agreement of the RCS results with both the pure MoM-VIE ($N_{tot}^{VIE}=15{,}360$, $T_{tot}^{VIE}=2{,}999\,s$, $M_{tot}^{VIE}=3.77\,GB$) and MoM-SIE solutions is, as can be observed from Fig. 4(b), again excellent, and the computation time with the diakoptic method is reduced by 17.2 times and the memory consumption by 24.8 times when compared to the MoM-VIE method. The MoM-SIE simulation requires

$N_{\text{tot}}^{\text{SIE}} = 6{,}144$, $T_{\text{tot}}^{\text{SIE}} = 333$ s, and $M_{\text{tot}}^{\text{SIE}} = 604$ MB.

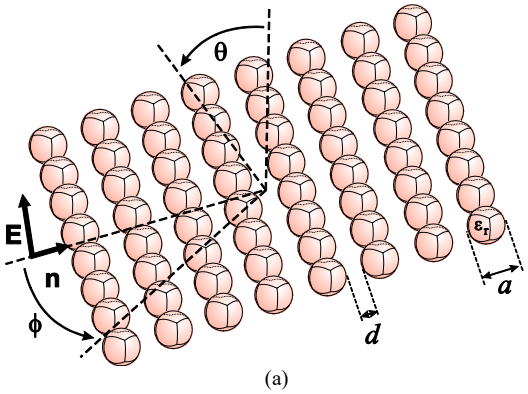

(a)

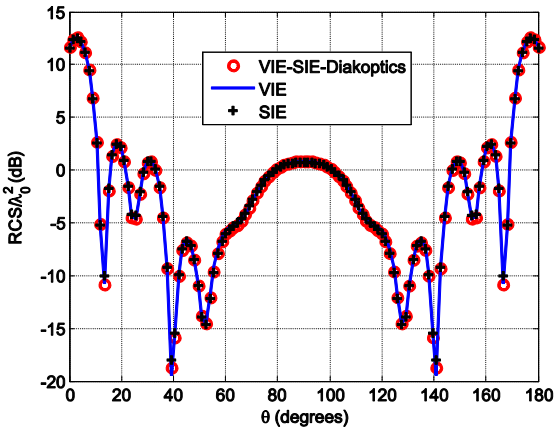

(b)

Fig. 4. (a) Array of homogeneous dielectric spherical scatterers excited by a uniform plane wave ($\theta_{\text{inc}} = 90°$, $\phi_{\text{inc}} = 0°$) and (b) normalized bistatic RCS results in the $\phi = 90°$ cut, obtained by the VSIE-diakoptic, pure MoM-VIE, and pure MoM-SIE method.

C. Array of Continuously Inhomogeneous Spherical Scatterers

As an example of inhomogeneous structures, that are also curved, we next consider a 4×4 array of continuously inhomogeneous dielectric spherical scatterers of diameters $a = \lambda_0/1.5$, shown in Fig. 5(a). All sphere-to-sphere distances are $d = \lambda_0/3$ and $\theta_{\text{inc}} = 0°$ and $\phi_{\text{inc}} = 0°$ for the impinging uniform plane wave. The inhomogeneity consists of a linear radial variation of the relative permittivity from $\varepsilon_r = 1$ at the surface to $\varepsilon_r = 6$ at the center of the spheres, as depicted in the inset of Fig. 5(b). Each scatterer is modeled by seven curvilinear hexahedral VIE elements (with $K_u = K_v = K_w = 2$), one element (with $N_u = N_v = N_w = 2$) approximating the central sphere (of diameter $a/20$) and six continuously inhomogeneous cushion-like elements (with $N_u = N_v = N_w = 3$) attached to the central element across the six corresponding sides, which can be seen in Fig. 5(a).

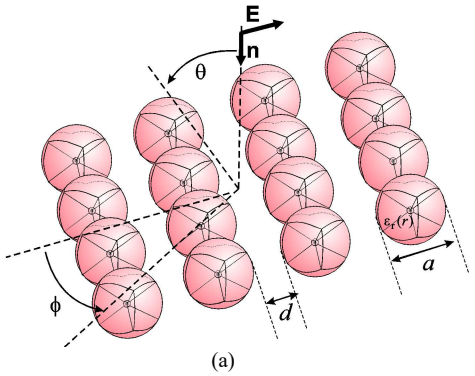

(a)

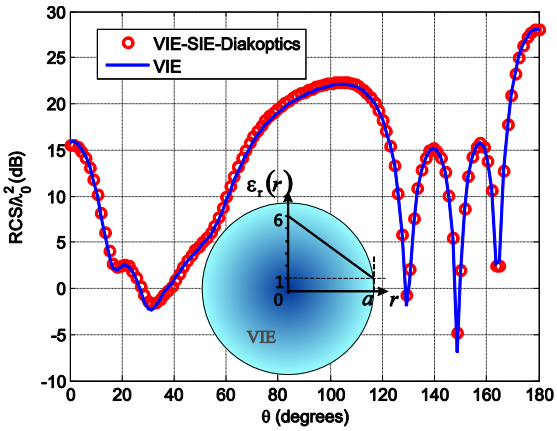

(b)

Fig. 5. (a) Array of continuously inhomogeneous dielectric spherical scatterers and (b) bistatic RCS results in the $\phi = 90°$ cut obtained by the VSIE-diakoptic and pure MoM-VIE methods.

The diakoptic surface enclosing each subsystem consists of six SIE patches with $K_u = K_v = 2$ and $N_u = N_v = 4$. The resulting numbers of unknowns are $N_{\text{V}} = 630$ (per subsystem), $2N_{\text{S}} = 6{,}144$ (total), and $N_{\text{tot}}^{\text{Dia}} = 6{,}774$, and the total computation time is $T_{\text{tot}}^{\text{Dia}} = 306$ s. In Fig. 5(b), an excellent agreement of the RCS calculated using the diakoptic method and the results obtained by the pure MoM-VIE method, with $N_{\text{tot}}^{\text{VIE}} = 10{,}080$ and $T_{\text{tot}}^{\text{VIE}} = 23{,}983$ s, is observed. In this case, the acceleration is even more dramatic (about 78.4 times) than in previous examples, because the MoM-VIE computation of matrix entries for a subsystem involving several inhomogeneous hexahedra is considerably more time consuming than for subsystems with a single homogeneous element. The required RAM for the VSIE-diakoptic and MoM-VIE solutions is $M_{\text{tot}}^{\text{Dia}} = 162$ MB and $M_{\text{tot}}^{\text{VIE}} = 1.6$ GB, respectively.

D. Diakoptic Decomposition of a Large Dielectric Slab

As an example of a single solid object decomposed into diakoptic subsystems, consider scattering from a dielectric slab with relative permittivity $\varepsilon_r = 2.25$ and dimensions $6\lambda_d \times 6\lambda_d \times 2\lambda_d$, with λ_d standing for the wavelength in the dielectric. The plane wave excitation is as in the previous

examples ($\theta_{inc} = 90°$, $\phi_{inc} = 0°$). The slab is decomposed into nine cubical diakoptic subsystems of edge lengths $d = 2\lambda_d$, as shown in Fig. 6(a). A single VIE element is used for each subsystem, with $K_u = K_v = K_w = 1$ and $N_u = N_v = N_w = 9$ ($N_V = 2{,}430$ per subsystem); it is enclosed by a six-patch diakoptic surface, with $K_u = K_v = 1$ and $N_u = N_v = 6$ (total of $2N_S = 7{,}776$ diakoptic unknowns). Note that the common surface between the neighboring diakoptic subsystems is taken into account by finding the limit of SIE integrals for the case when two (diakoptic) surfaces are infinitesimally close.

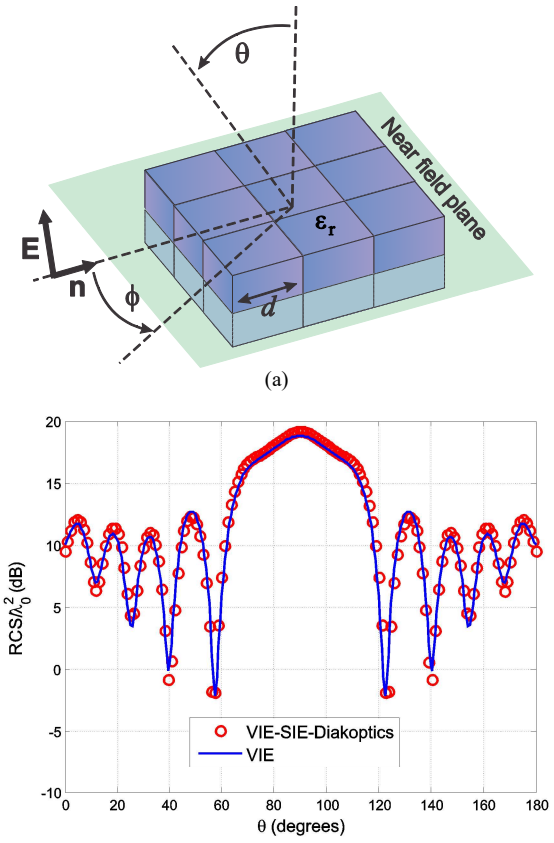

Fig. 6. (a) Large dielectric slab decomposesd into nine diakoptic subsystems and (b) comparison of the VSIE-diakoptic solution for the normalized bistatic RCS, in the $\phi = 0°$ cut, of the slab with results obtained using the pure MoM-VIE method.

In Fig. 6(b), we observe an excellent agreement of the VSIE-diakoptic RCS results for the dielectric slab ($N_{tot}^{Dia} = 10{,}206$, $T_{tot}^{Dia} = 118$ s, $M_{tot}^{Dia} = 373$ MB) with the solution obtained by the pure MoM-VIE method with $N_u = N_v = N_w = 9$ ($N_{tot}^{VIE} = 21{,}708$, $T_{tot}^{VIE} = 3{,}291$ s, $M_{tot}^{VIE} = 7.5$ GB). Hence the diakoptic method is 27.9 times faster and 20.2 times less expensive at memory consumption than the pure MoM approach in this case. For additional validation of the proposed diakoptic method, Fig. 7 shows the near (internal or external) total electric field computed in the plane indicated in Fig. 6(a). The VSIE-diakoptic results are compared with a pure-MoM-SIE solution ($N_{tot}^{SIE} = 3{,}936$, $T_{tot}^{SIE} = 68$ s, $M_{tot}^{SIE} = 248$ MB), and we observe an excellent agreement. As expected, the SIE solution, with modeling only the external, dielectric-air, surface of the slab in Fig. 6(a) and no unknowns for modeling the internal boundary surfaces between the adopted diakoptic subsystems, as well as no volume unknowns, is more efficient than the VSIE-diakoptic solution in this example. Note, however, that the results in this example and all other examples in this paper are aimed to demonstrate considerably higher efficiency of the VSIE-diakoptic method when compared to the pure MoM-VIE technique implementing the same discretization, with the pure MoM-SIE method serving just for validation and its numerical performance parameters being given for reference.

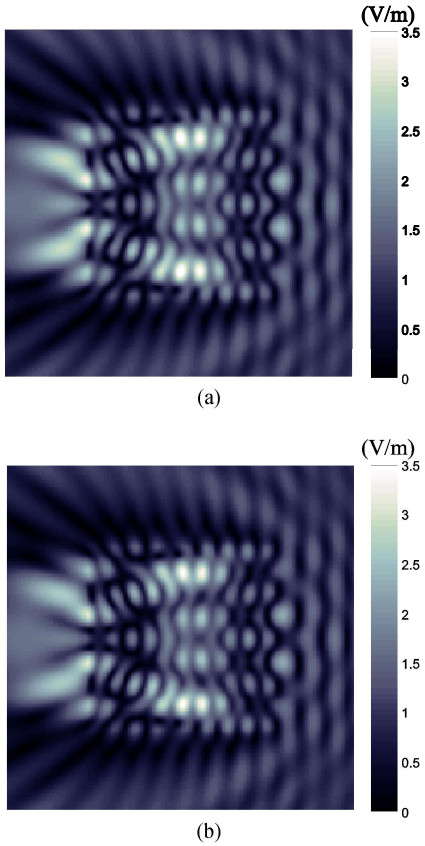

Fig. 7. Magnitude of the near total electric field inside and around the dielectric slab scatterer computed in the plane indicated in Fig. 6(a), where the size of the near-field computation area is $11\lambda_d \times 11\lambda_d$, and it cuts through the middle of the vertical dimension of the slab: comparison of (a) VSIE-diakoptic results and (b) pure MoM-SIE reference solution.

E. Diakoptic Decomposition of a Human Phantom

Finally, as an example of a complex object decomposed into completely different subsystems, consider scattering from a human phantom. The excitation of the phantom is by a uniform plane wave incident along the *x*-direction ($\theta_{inc} = 90°$, $\phi_{inc} = 0°$) at a frequency of 900 MHz, and the averaged equivalent complex relative permittivity of the homogeneous lossy dielectric material filling the phantom at this frequency is taken to be $\varepsilon_{rc} = 52.72 - j19.66$. The phantom is

decomposed into four diakoptic subsystems as shown in the inset of Fig. 8. Subsystems are different (the phantom is not symmetric) and are modeled by 1436, 1310, 1050, and 985 VIE hexahedra and 1124, 1114, 1018, and 976 SIE quadrilaterals, respectively (a total of $2N_S = 16{,}928$ diakoptic unknowns). Initial triangular mesh, provided by NEVA Electromagnetics [42], is re-meshed in ANSYS ICEM CFD 15.0.

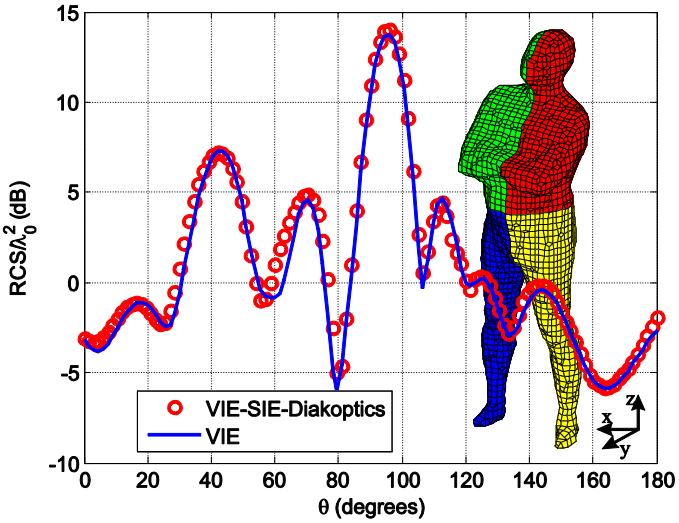

Fig. 8. Analysis of a human phantom decomposed into four diakoptic subsystems (figure inset): comparison of the VSIE-diakoptic solution for the normalized bistatic RCS ($\phi = 0^\circ$ cut) of the phantom with results obtained using the pure MoM-VIE method.

In Fig. 8, a good agreement of the VSIE-diakoptic RCS results for the human phantom ($N_{\text{tot}}^{\text{Dia}} = 33{,}387$, $T_{\text{tot}}^{\text{Dia}} = 17{,}584$ s, $M_{\text{tot}}^{\text{Dia}} = 3.7$ GB) with the pure MoM-VIE solution ($N_{\text{tot}}^{\text{VIE}} = 16{,}012$, $T_{\text{tot}}^{\text{VIE}} = 135{,}256$ s, $M_{\text{tot}}^{\text{VIE}} = 4.1$ GB) is observed. Hence, the acceleration gained with diakoptics in this example is 7.7 times, and because of the requirement for storage of all four different subsystem matrices, the reduction in RAM consumption is only 11%. Note that the number of VIE unknowns for the full system ($N_{\text{tot}}^{\text{VIE}}$) is smaller than the number of diakoptic unknowns, $2N_S = 16{,}928$. In this example, there are two advantages of the VSIE-diakoptics approach. On one hand, in diakoptics, the largest matrix that has to be LU decomposed is of size $N_S = 8{,}464$ (see Appendix I). On the other, the burdensome computation of the interaction of VIE elements belonging to different subsystems is replaced with faster computation of interaction between diakoptic surfaces.

IV. Conclusions

This paper has proposed a novel diakoptic method for 3-D electromagnetic analysis based on MoM-VSIE modeling. The method breaks the original structure into a number of non-overlapping closed-region subsystems (which may be the same or different) containing inhomogeneous dielectric materials and an open-region subsystem that encloses all other subsystems. Each subsystem is analyzed completely independently applying the double-higher-order large-domain Galerkin generalized MoM-VSIE or MoM-SIE solvers, and the final solution is obtained from diakoptic matrices expressing linear relations between electric and magnetic equivalent surface current coefficients on diakoptic surfaces.

The proposed VSIE-diakoptic method has been demonstrated, evaluated, and discussed in several characteristic examples, including both homogeneous and continuously inhomogeneous dielectric structures, objects with both flat surfaces/sharp edges and pronounced curvature, and both far-field and near-field computations. Numerical examples have demonstrated that the proposed VSIE-diakoptic method substantially increases the efficiency of the conventional pure MoM-VIE approach, with the pure MoM-SIE method serving for validation, as a very different technique. When compared to the pure MoM-VIE technique implementing the same type of discretization, the diakoptic approach enables considerable accelerations and memory savings, while fully preserving the accuracy of the analysis. The paper has also demonstrated that the general diakoptic methodology can effectively include VIE-based subsystems and has shown how that can be done.

Appendix I

A. Theoretical Analysis of Computational Complexity and Acceleration of VSIE-Diakoptics

Here, we make a theoretical estimate for the maximum efficiency of the diakoptic analysis, as compared to the standard MoM-VIE analysis, assuming single-level decomposition. We also assume that it is possible to subdivide the EM system into M congruent (i.e., geometrically identical) diakoptic subsystems, which differ only in their (physical) position in the original system and are analyzed by the generalized VSIE method. These subsystems are "wrapped" with a total of MN_D unknowns, namely, each subsystem has $N_D = 2N_S$ SIE unknowns on its surface, with N_S standing for the number of unknown coefficients for expansion of each of the equivalent currents $\mathbf{J}_e$ and $\mathbf{M}_e$ on the surface. Every VIE subsystem has N_V volumetric unknowns for the approximation of the displacement vector $\mathbf{D}$, so the total of VIE unknowns is MN_V. We assume, further, classical MoM codes, which utilize a direct solver based on LU factorization, so that the matrix filling and matrix solution have computational time complexities of $O(N^2)$ and $O(N^3)$, respectively, where N is the size of the matrix. Hence, the total analysis time of the entire VIE problem solved at once is given by $T_{\text{tot}}^{\text{VIE}} = k_V (MN_V)^2 + k^{\text{solv}} (MN_V)^3$, with k_V and k^{solv} standing for averaged times spent for each procedure per unknown coefficient. The total VIE filling and solution times are $k_V N_V^2$ and $k^{\text{solv}} N_V^2$, and those for the SIE are $k_S N_D^2$ and $k^{\text{solv}} N_D^2$, respectively. Therefore, the filling time for each

VSIE subsystem matrix can be computed as $k_{\mathrm{V}}^{\mathrm{sub}} N_{\mathrm{V}}^2 + k_{\mathrm{S}}^{\mathrm{sub}} N_{\mathrm{D}}^2 + 2k_{\mathrm{VS}}^{\mathrm{sub}} N_{\mathrm{V}} N_{\mathrm{D}}$, where $k_{\mathrm{S}}^{\mathrm{sub}}$, $k_{\mathrm{VS}}^{\mathrm{sub}}$, and $k_{\mathrm{V}}^{\mathrm{sub}}$ are averaged times spent per computation of the corresponding matrix element in the subsystem.

In the proposed VSIE-diakoptic approach, matrices to be computed are of sizes $N_{\mathrm{D}} + N_{\mathrm{V}}$ and MN_{D}, and the sizes of matrices that need to be solved are MN_{S} and $N_{\mathrm{V}} + N_{\mathrm{S}}$. Taking into account that $k_{\mathrm{S}}^{\mathrm{sub}} << k_{\mathrm{VS}}^{\mathrm{sub}} << k_{\mathrm{V}}^{\mathrm{sub}}$ (since $k_{\mathrm{S}}^{\mathrm{sub}}$, $k_{\mathrm{VS}}^{\mathrm{sub}}$, and $k_{\mathrm{V}}^{\mathrm{sub}}$ are essentially the times required for surface-surface, surface-volume, and volume-volume integration, respectively), the total time needed for the diakoptic analysis is

$$T_{\mathrm{tot}}^{\mathrm{Dia}} \approx \max\left\{k_{\mathrm{V}}^{\mathrm{sub}} N_{\mathrm{V}}^2, k_{\mathrm{S}}\left(2MN_{\mathrm{S}}\right)^2\right\} + k^{\mathrm{solv}}\left[2\left(MN_{\mathrm{S}}\right)^3 + \left(N_{\mathrm{V}} + N_{\mathrm{S}}\right)^3\right]. \quad (15)$$

Note that $k_{\mathrm{V}}^{\mathrm{sub}} \neq k_{\mathrm{V}}$, which is because the computation of matrix elements obtained via integration of basis functions belonging to the same element or neighboring elements requires more time than for those related to the distant elements. In our numerical code, the average filling time of the entire VIE system is related to the time for its subsystem as $k_{\mathrm{V}}^{\mathrm{sub}} = k_{\mathrm{V}} \sqrt[3]{M}$.

Based on the above, the theoretically maximum acceleration of the VSIE-diakoptics as compared to the standard MoM-VIE analysis can be estimated as

$$\frac{T_{\mathrm{tot}}^{\mathrm{VIE}}}{T_{\mathrm{tot}}^{\mathrm{Dia}}} \approx \frac{k_{\mathrm{V}}\left(MN_{\mathrm{V}}\right)^2 + k^{\mathrm{solv}}\left(MN_{\mathrm{V}}\right)^3}{T_{\mathrm{fill}}^{\mathrm{Dia}} + k^{\mathrm{solv}}\left[2\left(MN_{\mathrm{S}}\right)^3 + \left(N_{\mathrm{V}} + N_{\mathrm{S}}\right)^3\right]}, \quad (16)$$

where $T_{\mathrm{fill}}^{\mathrm{Dia}} = \max\{k_{\mathrm{V}} \sqrt[3]{M} N_{\mathrm{V}}^2, k_{\mathrm{S}}\left(2MN_{\mathrm{S}}\right)^2\}$ is the time required for filling of all diakoptic matrices, computed simultaneously. Additionally, (16) can be generalized to predict acceleration of the system subdivided into non-congruent subsystems. In such a case, $T_{\mathrm{fill}}^{\mathrm{Dia}}$ is the maximum of all anticipated filling times for the diakoptic matrices. Table I gives the actually measured and theoretically maximum acceleration values for all examples in the paper, in Sections III.A–E.

Note that the anticipated theoretical acceleration in (16) is the maximum acceleration that can possibly be achieved, by the respective system subdivision using a given numerical VSIE-diakoptic code. The actual acceleration is lower, due to the fact that the computation time $T_{\mathrm{tot}}^{\mathrm{Dia}}$ does not include times required for preprocessing, post-processing, and matrix assembly (summation of diakoptic subsystem sub-matrices and row/column manipulations), as well as the $k_{\mathrm{S}}^{\mathrm{sub}} N_{\mathrm{D}}^2 + 2k_{\mathrm{VS}}^{\mathrm{sub}} N_{\mathrm{V}} N$ portion of the subsystem matrix filling time. However, despite of all these omissions and simplifications, the simple formula in (16) provides, as can be observed from Table I, a good estimate of the efficiency of the diakoptic performance. Namely, all actually measured acceleration values agree well with the corresponding theoretically maximum values in Table I – for all examples in the paper.

We also observe from Table I considerable (measured and theoretical) accelerations, while fully preserving the accuracy of the analysis, enabled by the diakoptic approach when compared to the pure MoM-VIE technique implementing the same type of discretization, in all examples in Sections III.A–E.

TABLE I
ACTUALLY MEASURED AND THEORETICALLY MAXIMUM ACCELERATION

Example in Sections III.A–E	Measured Acceleration	Theoretically Max. Acceleration
Array of Homogeneous Dielectric Cubical Scatterers	4.5	5.9
Array of Homogeneous Dielectric Spherical Scatterers	17.2	20.1
Array of Continuously Inhomogeneous Spherical Scatterers	78.4	95.1
Diakoptic Decomposition of a Large Dielectric Slab	27.9	31.3
Diakoptic Decomposition of a Human Phantom	7.7	9.4

REFERENCES

[1] J. L. Volakis and K. Sertel, *Integral Equation Methods for Electromagnetics*, SciTech Publishing, 2012.

[2] B.M. Kolundžija and A.R. Djordjević, *Electromagnetic modeling of composite metallic and dielectric structures*, Boston: Artech House, 2002.

[3] S. Omar and D. Jiao, "A new volume integral formulation for broadband 3-D circuit extraction in inhomogeneous materials with and without external electromagnetic fields," *IEEE Transactions on Microwave Theory and Techniques*, vol. 61, No. 12, pp. 4302-4312, December 2013.

[4] M. S. Tong, Y. Q. Zhang, R. P. Chen, and C. X. Yang, "Fast solutions of volume integral equations for electromagnetic scattering by large highly anisotropic objects," *IEEE Transactions on Microwave Theory and Techniques*, vol. 62, No. 7, pp. 1429-1436, July 2014.

[5] S. Omar and D. Jiao, "A linear complexity direct volume integral equation solver for full-wave 3-D circuit extraction in inhomogeneous materials," *IEEE Transactions on Microwave Theory and Techniques*, vol. 63, No. 3, pp. 897-912, March 2015.

[6] E. Chobanyan, M. M. Ilić, and B. M. Notaroš, "Double-higher-order large-domain volume/surface integral equation method for analysis of composite wire-plate-dielectric antennas and scatterers," *IEEE Transactions on Antennas and Propagation*, vol. 61, No. 12, pp. 6051-6063, December 2013.

[7] M. Djordjević and B. M. Notaroš, "Double higher order method of moments for surface integral equation modeling of metallic and dielectric antennas and scatterers," *IEEE Transactions on Antennas and Propagation*, vol. 52, No. 8, pp. 2118-2129, August 2004.

[8] B. C. Usner, K. Sertel, M. A. Carr, and J. L. Volakis, "Generalized volume-surface integral equation for modeling inhomogeneities within high contrast composite structures," *IEEE Transactions on Antennas and Propagation*, vol. 54, No.1, pp. 68-75, January 2006.

[9] E. Chobanyan, M. M. Ilić, and B. M. Notaroš, "Scattering analysis using generalized volume-surface integral equation method of moments"

Proceedings of 2014 IEEE Antennas and Propagation Society International Symposium, Memphis, Tennessee, July 6-12, 2014.

[10] G. Kron, *Diakoptics: The Piecewise Solution of Large Scale Systems*, MacDonald, 1963.

[11] D. I. Olćan, I. M. Stevanović, J. R. Mosig, and A. R. Djordjević, "Diakoptic approach to analysis of multiconductor transmission lines," *Microwave and Optical Technology Letters*, vol. 50, No. 4, pp. 931-936, April 2008.

[12] D. I. Olćan, I. M. Stevanović, B. M. Kolundžija, J. R. Mosig, and A. R. Djordjević, "Diakoptic surface integral-equation formulation applied to large antenna arrays," *Proceedings of 2008 IEEE Antennas and Propagation Society International Symposium*, San Diego, CA, July 4-12, 2008.

[13] A. B. Manić, D. I. Olćan, M. M. Ilić, and B. M. Notaroš, "Diakoptic approach combining finite element method and method of moments in analysis of inhomogeneous anisotropic dielectric and magnetic scatterers," *Special Issue on Finite Elements for Microwave Engineering*, *Electromagnetics*, vol. 34, Issue 3-4, April 2014, pp. 222-238.

[14] E. Chobanyan, D. I. Olćan, M. M. Ilić, and B. M. Notaroš, "Combining diakoptic, VIE-MoM, and SIE-MoM approaches in analysis of dielectric scatterers," *Proceedings of 2013 IEEE Antennas and Propagation Society International Symposium*, Orlando, Florida, July 7-12, 2013.

[15] M.-K. Li and W. C. Chew, "Wave-field interaction with complex structures using equivalence principle algorithm," *IEEE Transactions on Antennas and Propagation*, vol. 55, No. 1, pp. 130-138, January 2007.

[16] M.-K. Li and W. C. Chew, "Multiscale simulation of complex structures using equivalence principle algorithm with high-order field point sampling scheme," *IEEE Transactions on Antennas and Propagation*, vol. 56, No. 8, pp. 2389-2397, August 2008.

[17] P. Yla-Oijala and M. Taskinen, "Electromagnetic scattering by large and complex structures with surface equivalence principle algorithm," *Waves in Random and Complex Media*, vol. 19, pp. 105-125, February 2009.

[18] M.-K. Li, W.C. Chew, and L.J. Jiang, "Domain decomposition scheme based on equivalence theorem," *Microwave and Optical Technology Letters*, vol. 48, No. 9, pp. 1853-1857, September 2006.

[19] W. C. Chew and C. C. Lu, "The use of Huygens' equivalence principle for solving the volume integral equation of scattering," *IEEE Transactions on Antennas and Propagation*, vol. 41, No. 7, pp. 897-904, July 1993.

[20] C. C. Lu and W. C. Chew, "The use of Huygens' equivalence principle for solving 3-D volume integral equation of scattering," *IEEE Transactions on Antennas and Propagation*, vol. 43, No. 5, pp. 500-507, May 1995.

[21] S.-C. Lee, M. N. Vouvakis, and J.-F. Lee, "A nonoverlapping domain decomposition method with nonmatching grids for modeling large finite antenna arrays," *Journal of Computational Physics*, vol. 203, pp. 1–21, February 2005.

[22] Y. J. Li and J. M. Jin, "A vector dual-primal finite element tearing and interconnecting method for solving 3-D large-scale electromagnetic problems," *IEEE Transactions on Antennas and Propagation*, vol. 54, No. 10, pp. 3000–3009, October 2006.

[23] V. de la Rubia and J. Zapata, "Microwave circuit design by means of direct decomposition in the finite-element method," *IEEE Transactions on Microwave Theory and Techniques*, vol. 55, No. 7, pp. 1520-1530, July 2007.

[24] Y. J. Li and J. M. Jin, "A new dual-primal domain decomposition approach for finite element simulation of 3-D large-scale electromagnetic problems," *IEEE Transactions on Antennas and Propagation*, vol. 55, No. 10, pp. 2803-2810, October 2007.

[25] S.-H. Lee and J. M. Jin, "Efficient full-wave analysis of multilayer interconnection structures using a novel domain decomposition–model-order reduction method," *IEEE Transactions on Microwave Theory and Techniques*, vol. 56, No. 1, pp. 121-130, January 2008.

[26] K. Zhao, V. Rawat, and J.-F. Lee, "A domain decomposition method for electromagnetic radiation and scattering analysis of multi-target problems," *IEEE Transactions on Antennas and Propagation*, vol. 56, No. 8, pp. 2211-2221, August 2008.

[27] Y. Shao, Z. Peng, and J.-F. Lee, "Full-wave real-life 3-D package signal integrity analysis using nonconformal domain decomposition method," *IEEE Transactions on Microwave Theory and Techniques*, vol. 59, No. 2, pp. 230-241, February 2011.

[28] L. Yin, J. Wang, and W. Hong, "A novel algorithm based on the domain-decomposition method for the full-wave analysis of 3-D electromagnetic problems," *IEEE Transactions on Microwave Theory and Techniques*, vol. 50, No. 8, pp. 2011-2017, August 2002.

[29] F. Xu, K. Wu, and W. Hong, "Domain decomposition FDTD algorithm combined with numerical TL calibration technique and its application in parameter extraction of substrate integrated circuits," *IEEE Transactions on Microwave Theory and Techniques*, vol. 54, No. 1, pp. 329-338, January 2006.

[30] Z. Peng, X.-C. Wang, and J.-F. Lee, "Integral equation based domain decomposition method for solving electromagnetic wave scattering from non-penetrable objects," *IEEE Transactions on Antennas and Propagation*, vol. 59, No. 9, pp. 3328-3338, September 2011.

[31] Z. Peng, K.-H. Lim, and J.-F. Lee, "Computations of electromagnetic wave scattering from penetrable composite targets using a surface integral equation method with multiple traces," *IEEE Transactions on Antennas and Propagation*, vol. 61, No. 1, pp. 256-270, January 2013.

[32] R. F. Harrington, *Time-Harmonic Electromagnetic Fields*. New York: John Wiley & Sons, 2001.

[33] H. Guo, J. Hu, and E. Michielssen, "On MLMDA/butterfly compressibility of inverse integral operators," *IEEE Antennas and Wireless Propagation Letters*, Vol. 12, pp. 31-34, 2013.

[34] Y. Brick, V. Lomakin, and A. Boag, "Fast direct solver based on the generalized equivalence integral equation," *Proceedings of 2013 URSI International Symposium on Electromagnetic Theory (EMTS)*, pp. 614-617, May 20-24, 2013.

[35] S. Omar and D. Jiao, "O(N) iterative and O(NlogN) direct volume integral equation solvers for large-scale electrodynamic analysis," *Proceedings of 2014 International Conference on Electromagnetics in Advanced Applications (ICEAA)*, pp.593-596, Aug. 3-8, 2014.

[36] K. Sertel, and J. L. Volakis, " Multilevel fast multipole method solution of volume integral equations using parametric geometry modeling," *IEEE Transactions on Antennas and Propagation*, vol. 52, No.7, pp. 1686-1692, July 2004.

[37] X.-C. Nie, N. Yuan, L.-W. Li, Y.-B. Gan, and T. S. Yeo, " A fast combined field volume integral equation solution to EM scattering by 3-D dielectric objects of arbitrary permittivity and permeability," *IEEE Transactions on Antennas and Propagation*, vol. 54, No.3, pp. 961-969, March 2006.

[38] S. Jarvenpaa, J. Markkanen, and P. Yla-Oijala, " Broadband Multilevel Fast Multipole Algorithm for Electric-Magnetic Current Volume Integral Equation," *IEEE Transactions on Antennas and Propagation*, vol. 61, No.8, pp. 4393 - 4397, May 2013.

[39] Z. Qian, W. C. Chew, and R. Suaya, "Generalized impedance boundary condition for conductor modeling in surface integral equation," *IEEE Transactions on Microwave Theory and Techniques*, vol. 55, no. 11, pp. 2354–2364, 2007.

[40] S. He, W. E. I. Sha, L. Jiang, W. C. H. Chou, W. C. Chew, and Z. Nie, "Finite-element-based generalized impedance boundary condition for modeling plasmonic nanostructures," *IEEE Transactions on Nanotechnology*, vol. 11, no. 2, pp. 336–345, 2012.

[41] M. Paz and W. Leigh, *Integrated Matrix Analysis of Structures Theory and Computation*, Kluwer Academic Publishers, 2001.

[42] G. Noetscher, A. T. Htet, and S. Makarov, "N-Library of basic triangular surface human body meshes from male subjects," *NEVA Electromagnetics LLC*, October 2012.

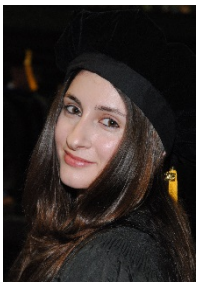

Elene Chobanyan (S'12-M'16) was born in Tbilisi, Georgia, in 1986. She received the B.S. degree in physics and the M.S. degree in electrical and electronics engineering from Tbilisi State University, Tbilisi, Georgia, in 2007 and 2009, respectively, and PhD. Degree in electrical and computer engineering from Colorado State University, USA, in 2015.

From 2006 to 2010, she worked in the R&D department at EMCoS in Tbilisi, Georgia. As a member of EM Methods Development Department, she was primarily dealing with computational techniques such as Method of Moments (MoM), Method of Auxiliary Sources (MAS), Transmission Line Methods and Network Analysis. In 2008 she was an EMCoS representative at "JSOL Corporation"

(former JRI Solutions, Ltd.) in Tokyo, Japan. In summer 2013 she was an intern in engineering simulation software developer ANSYS Inc. in Boulder, Colorado. Since 2015, she has been working as a Signal Integrity Engineer at CDI HW Platform R&D at Hewlett Packard Enterprise in Fort Collins, Colorado. Her research interests include computational electromagnetics, domain decomposition techniques, high speed PCB design, non-volatile and volatile memory systems, computer architecture, and electromagnetic interference.

Dragan I. Olćan (S'05-M'09) is an Associate Professor at the School of Electrical Engineering, University of Belgrade, Serbia, where he received his B.Sc. (5 years), M.Sc., and Ph.D. degrees in 2001, 2004, and 2008, respectively. He is a coauthor of three commercial electromagnetic software codes, eleven journal papers, more than sixty conference papers, and five university textbooks. His main research interests are: numerical electromagnetic analysis including domain decomposition, optimization algorithms applied to electromagnetic designs, and electromagnetic compatibility testing.

Milan M. Ilić (S'00–M'04) received the Dipl. Ing. and M.S. degrees in Electrical Engineering from the University of Belgrade, Serbia, in 1995 and 2000, respectively, and the Ph.D. degree from the University of Massachusetts Dartmouth, USA, in 2003.

He is currently an Associate Professor in the School of Electrical Engineering at the University of Belgrade and a postdoctoral Research Associate and Affiliated Faculty with the ECE department of the Colorado State University, USA. His research interests include computational electromagnetics, antennas, and microwave electronics.

Dr. Ilić was the recipient of the 2005 IEEE MTT-S Microwave Prize.

Branislav M. Notaroš (M'00-SM'03-F'16) was born in Zrenjanin, Yugoslavia, in 1965. He received the Dipl.Ing. (B.S.), M.S., and Ph.D. degrees in electrical engineering from the University of Belgrade, Belgrade, Yugoslavia, in 1988, 1992, and 1995, respectively.

From 1996 to 1999, he was an Assistant Professor in the School of Electrical Engineering at the University of Belgrade. He spent the 1998-1999 academic year as a Visiting Scholar at the University of Colorado at Boulder. He was an Assistant Professor, from 1999 to 2004, and Associate Professor, from 2004 to 2006, in the Department of Electrical and Computer Engineering at the University of Massachusetts Dartmouth. From 2006 to 2012, he was an Associate Professor in the Department of Electrical and Computer Engineering at Colorado State University, where he is currently a Professor and University Distinguished Teaching Scholar, as well as Director of Electromagnetics Laboratory. His research interests and activities are in computational electromagnetics, higher order numerical methods, antennas, scattering, microwaves, metamaterials, characterization of snow and rain, surface and radar precipitation measurements, RF design for MRI at ultra-high magnetic fields, and electromagnetics education. His publications include more than 180 journal and conference papers, and three workbooks in electromagnetics and in fundamentals of electrical engineering (basic circuits and fields). He is the author of textbooks *Electromagnetics* (Prentice Hall, 2010), *MATLAB-Based Electromagnetics* (Prentice Hall, 2013), and *Conceptual Electromagnetics* (CRC Press, 2016).

Dr. Notaroš is Fellow of IEEE. He served as General Chair for the 11th International Workshop on Finite Elements for Microwave Engineering – FEM2012, June 4-6, 2012, Estes Park, Colorado, USA, and as Guest Editor of the Special Issue on Finite Elements for Microwave Engineering, Electromagnetics, Vol. 34, Issue 3-4, 2014. He serves on the Board of Directors of the Applied Computational Electromagnetics Society (ACES) (2016-2019) and as Chair of the Technical Committee for the Commission B of the US National Committee, International Union of Radio Science (URSI) (since 2014). He was the recipient of the 2005 IEEE MTT-S Microwave Prize (best-paper award for IEEE Transactions on MTT), 1999 IEE Marconi Premium (best-paper award for IEE Proceedings on Microwaves, Antennas and Propagation), 1999 URSI Young Scientist Award, 2005 UMass Dartmouth Scholar of the Year Award, 2004 UMass Dartmouth College of Engineering Dean's Recognition Award, 1992 Belgrade Chamber of Industry and Commerce Best M.S. Thesis Award, 2009, 2010, 2011, and 2014 Colorado State University Electrical and Computer Engineering Excellence in Teaching Awards, 2010 Colorado State University College of Engineering George T. Abell Outstanding Teaching and Service Faculty Award, 2012 Colorado State University System Board of Governors Excellence in Undergraduate Teaching Award, 2014 Colorado State University Provost's N. Preston Davis Award for Instructional Innovation, 2012 IEEE Region 5 Outstanding Engineering Educator Award, 2014 Carnegie Foundation for the Advancement of Teaching Colorado Professor of the Year Award, 2015 American Society for Engineering Education ECE Distinguished Educator Award, and 2015 IEEE Undergraduate Teaching Award.